Available online at www.sciencedirect.com
ScienceDirect
Polymer 49 (2008) 922–933
polymer
www.elsevier.com/locate/polymer

Selective hydrogen bonding and hierarchical nanostructures in poly(hydroxyether of bisphenol A)/poly(ε-caprolactone)-*block*-poly(2-vinyl pyridine) blends

Nishar Hameed, Qipeng Guo*

Centre for Material and Fibre Innovation, Deakin University, Pigdons Road, Geelong, Victoria 3217, Australia

Received 21 November 2007; received in revised form 21 December 2007; accepted 23 December 2007
Available online 8 January 2008

Abstract

The phase behavior, hydrogen bonding interactions and morphology of poly(hydroxyether of bisphenol A) (phenoxy) and poly(ε-caprolactone)-*block*-poly(2-vinyl pyridine) (PCL-*b*-P2VP) were investigated using differential scanning calorimetry (DSC), Fourier transform infrared (FTIR) spectroscopy, optical microscopy and atomic force microscopy (AFM). In this A-*b*-B/C type block copolymer/homopolymer system, both P2VP and PCL blocks have favorable intermolecular interaction towards phenoxy via hydrogen bonding. However, the hydrogen bonding between P2VP and phenoxy is significantly stronger than that between PCL and phenoxy. Selective hydrogen bonding between phenoxy/P2VP pair at lower phenoxy contents and co-existence of two competitive hydrogen bonding interactions between phenoxy/P2VP and phenoxy/PCL pairs at higher phenoxy contents were observed in the blends. This leads to the formation of a variety of composition dependent nanostructures including wormlike, hierarchical and core–shell morphologies. The blends became homogeneous at 95 wt% phenoxy where both blocks of the PCL-*b*-P2VP were miscible with phenoxy due to hydrogen bonding. In the end, a model was proposed to explain the microphase morphology of blends based on the experimental results obtained. The swelling of the PCL-*b*-P2VP block copolymer by phenoxy due to selective hydrogen bonding causes formation of different microphases.

Keywords: Polymer blend; Block copolymer; Hydrogen bonding

1. Introduction

In multiphase polymer systems, the control of order on a mesoscopic length scale has become an important subject of interest, since polymers offer a way to construct ordered nanoscale domains through different ways, including the repulsion between different components, self-organization, competing intermolecular interactions, etc. [1–5]. This area has been stimulated by the urge to miniaturize devices for structural applications as well as their wide range of applications in advanced material formation, pollution control, drug delivery, etc. [6–9]. Among this, block copolymers are of particular interest due to their ability to form a rich variety of microstructures. A range of ordered structures can be created using block copolymers, depending on the number of blocks, their volume fraction, chain flexibility and the extent of repulsion between the chemically connected blocks. If the diblock components are incompatible, they can form different ordered morphologies including cylinders, lamellae, wormlike and spherical micelles [10,11]. The morphologies of a large number of blends containing a diblock copolymer and a homopolymer have been discussed by several authors [12–15]. In a diblock copolymer/homopolymer system, ordered structures can be established in different ways, including (1) the smectic order resulting from the covalently bonded mesogenic side groups and (2) the ordered microphase formation used by the secondary interactions such as hydrogen bonding, coordination bonding, ionic interactions, etc. [16]. Among these, the introduction of hydrogen bonding interactions into the block

* Corresponding author. Tel.: +61 3 5227 2802; fax: +61 3 5227 1103.
E-mail address: qguo@deakin.edu.au (Q. Guo).

0032-3861/$ - see front matter © 2008 Elsevier Ltd. All rights reserved.
doi:10.1016/j.polymer.2007.12.040

polymer blend systems provides a variety of new classes of self-assembling mechanisms of those molecules, which may lead to production of highly functional polymeric materials. This area is of great interest since this microphase-separated system can be used for the creation of hybrid or periodic nanoporous materials for potential applications by means of nanoparticle filling of the pores after the removal of one component. From the perspective of creation of ordered nanostructures, hierarchical structures have become increasingly interesting. Different highly ordered hierarchical structures have been achieved from complex block copolymer systems. Ruokolainen et al. [17] developed hierarchical structures with double periodicity in block copolymer/low molecular weight compound blend system. They blended pentadecylphenol with polystyrene–poly(4-vinyl pyridine) to obtain periodic lamellae-in-lamellae structure which are perpendicular to each other. Various micellar and core–shell morphologies, as well as morphologies in which the domain boundaries of lamellar or cylindrical morphologies have been decorated with a third phase, have been reported by several investigators [18].

Various studies have been conducted in A-*b*-B/C type block copolymer/homopolymer blends, wherein the Flory–Huggins interaction parameter (χ) between the interacting polymers (χ_{AC}, χ_{BC} or χ_{AB}) is either positive or negative [19]. Poly(styrene-*block*-isoprene)/poly(phenylene oxide) and poly(styrene-*block*-butadiene)/poly(methyl vinyl ether) blends were investigated by Hashimoto et al. [20,21], wherein the homopolymers exhibit negative χ parameters with polystyrene. Zhao et al. [22] conducted a variety of studies on the block copolymer poly(styrene)-*block*-poly(4-vinyl phenol) (PS-*b*-PVPh) with various homopolymers having both attractive and repulsive interactions with the block copolymer components. Blends of PS-*b*-PVPh with poly(vinyl methyl ether) (PVME) showed special behavior because PVME was known to be miscible with PS and PVPh blocks of the copolymer, i.e., both χ_{AC} and χ_{BC} are negative. They proved that PVME, if present in sufficient amount, can act as a common solvent for both of the blocks in the block copolymer.

In the present work, we investigate the selective hydrogen bonding in poly(hydroxyether of bisphenol A) (phenoxy)/poly(ε-caprolactone)-*block*-poly(2-vinyl pyridine) (PCL-*b*-P2VP) blends, wherein both the blocks are miscible with the phenoxy depending on the concentration of the latter. Here, the value of χ_{AB} is positive (A and B are immiscible), and χ_{AC} and χ_{BC} are negative, but χ_{BC} is more negative than χ_{AC}. PCL is a crystalline, non-associating polymer, which owes carbonyl group as proton accepting group. P2VP has a strong proton accepting capacity due to the nitrogen atom present in the pyridine ring. Miscible polymer blends of phenoxy/P2VP [23] and phenoxy/PCL [24,25] systems were reported by other authors. Consequently, phenoxy/PCL-*b*-P2VP mixture is expected to exhibit a high level of intermolecular hydrogen bonding due to the presence of both excellent proton donors and proton acceptors. From this point of view, we blended an amphiphilic diblock copolymer, PCL-*b*-P2VP, with phenoxy knowing that: (1) P2VP nitrogens and phenoxy hydroxyl groups can form very strong hydrogen bonds at any composition where the inter-association is much stronger than self-association in phenoxy and (2) PCL carbonyl groups can also form hydrogen bonds with phenoxy hydroxyl but the inter-association here is much weaker than the self-association in phenoxy. Therefore, it is expected that by blending we can selectively control the microphase separation of PCL blocks by varying composition while the P2VP blocks remain miscible with the phenoxy. As a consequence, the nanostructured blends can be prepared via selective solubility.

The effect of hydrogen bonding on the phase behavior was investigated using differential scanning calorimetry (DSC) and Fourier transform infrared (FTIR) spectroscopy. The semicrystalline morphology and microphase morphology of the blends were examined using polarizing optical microscopy (POM) and atomic force microscopy (AFM), respectively.

2. Experimental section

2.1. Materials and methods

The polymers used in the present study were poly(hydroxyether of bisphenol A) (phenoxy) and poly(ε-caprolactone)-*block*-poly(2-vinyl pyridine) (PCL-*b*-P2VP). Phenoxy, with an average $M_w = 40{,}000$, was obtained from Aldrich Chemical Company, Inc. The PCL-*b*-P2VP copolymer was from Polymer Sources, Inc., with M_n (P2VP) = 20,900, M_n (PCL) = 26,100 and $M_w/M_n = 1.11$. The polymers were used as received. The phenoxy/PCL-*b*-P2VP blends were prepared by solution mixing. Chloroform solution containing 1% (w/v) of the polymer mixture was stirred well until a clear solution was obtained. The solvent was allowed to evaporate slowly at room temperature. The blend samples were dried in vacuum at 80 °C for 24 h before the measurements.

2.2. Differential scanning calorimetry (DSC)

The thermal behavior of the blends was analyzed by a Perkin–Elmer Diamond DSC. The measurement was performed using 5–10 mg of the sample under an atmosphere of nitrogen gas. The samples were first heated to 100 °C and held at that temperature for 5 min to remove the thermal history. Then the samples were cooled to −50 °C at the rate of 20 °C/min, held for 5 min, and again heated from −50 to 150 °C at 20 °C/min (second scan). T_g values were taken as the midpoint of transition in the second scan of DSC thermograms.

2.3. Fourier transform infrared (FTIR) spectroscopy

The KBr disk method was adopted to determine the FTIR characteristics of the blends. The FTIR spectra of all the samples were measured on a Bruker Vetex-70 FTIR spectrometer. The chloroform sample solution was cast onto KBr disk, and the solvent was allowed to evaporate slowly at room temperature. The disks were dried under vacuum in an oven before the measurements. The spectra were recorded at the average of 32 scans in the standard wavenumber range of 400–4000 cm^{-1} at a resolution of 4 cm^{-1}.

2.4. Polarizing optical microscopy (POM)

The semicrystalline morphology of phenoxy/PCL-*b*-P2VP blends were analyzed using a Nikon eclipse-80*i* optical microscope under polarized light. The chloroform cast solutions of the blends were spread as thin films on the glass slides and dried in vacuum oven.

2.5. Atomic force microscopy (AFM)

The phase morphology of the blends was examined using an AFM (DME type DS 45-40, Denmark) in the tapping mode at room temperature. The thin films of the samples were prepared on glass slides. The height and phase images were recorded simultaneously while operating the instrument in the tapping mode.

3. Results and discussion

3.1. Hydrogen bonding interactions in the blends

FTIR spectroscopy has been used to prove the existence of hydrogen bonding interactions in the blends. Fig. 1 shows the possible hydrogen bonding interactions between phenoxy and PCL-*b*-P2VP blends. Infrared studies show that the hydroxyl, carbonyl and pyridine ring peaks undergo important changes, which can be attributed to the hydrogen bonding between them. The hydroxyl stretching region in the infrared spectra of phenoxy/PCL-*b*-P2VP blends at room temperature is given in Fig. 2. Phenoxy is a self-associating polymer due to the presence of pendant hydroxyl groups. Pure phenoxy shows two distinct bands in the hydroxyl region. A broad band centered at 3435 cm^{-1} and a shoulder band at 3564 cm^{-1}, which can be attributed to the stretching vibrations of self-associated hydroxyl groups and non-associated free hydroxyl groups, respectively. Upon the addition of the block copolymer, the peak corresponding to the free hydroxyl groups decreases in intensity and eventually disappears, whereas the hydrogen bonded band shifts towards the lower wavenumber region. The peak at 3398 cm^{-1} of 10/90 phenoxy/PCL-*b*-P2VP blends corresponds to the hydrogen bonding interaction between hydroxyl groups of phenoxy and pyridine and/or carbonyl groups of the block copolymer. It is noticed that the inter-associated

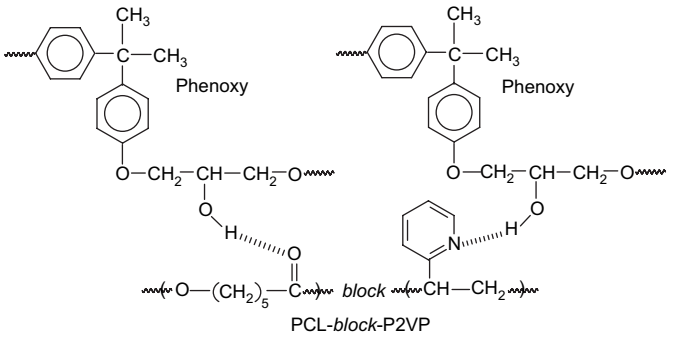

Fig. 1. Schematic representation of possible interactions between phenoxy and PCL-*b*-P2VP block copolymers.

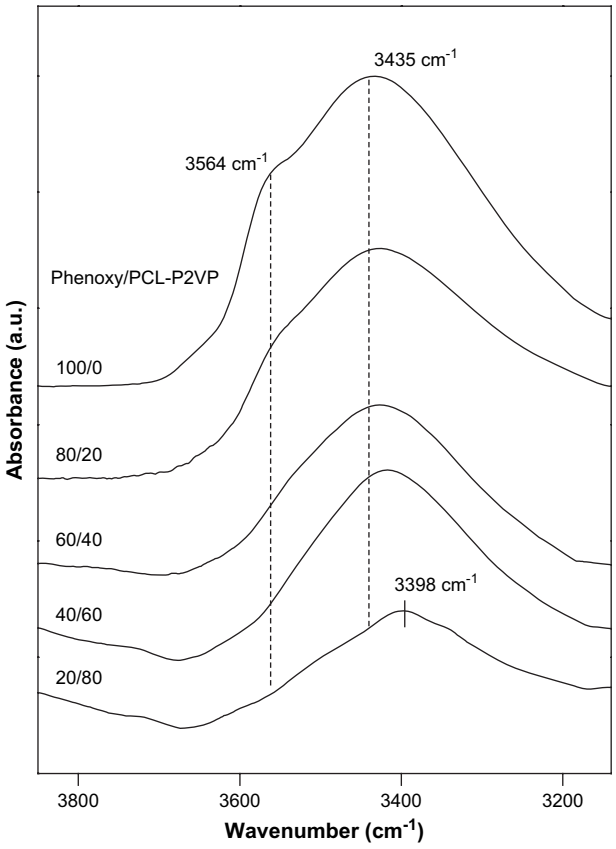

Fig. 2. Hydroxyl stretching region in the infrared spectra of phenoxy/PCL-*b*-P2VP blends at room temperature.

hydrogen bonds between phenoxy and PCL-*b*-P2VP are stronger than the self-associated hydrogen bonds in pure phenoxy. This result can be compared with those obtained for phenoxy/P2VP (or P4VP) and phenoxy/PCL binary blends investigated by other authors. de Ilarduya et al. [23] investigated that the inter-association hydrogen bonding in phenoxy/P2VP blends is much stronger than self-association in phenoxy. Coleman and Moskala [24] proved that PCL/phenoxy blends exhibited FTIR peaks corresponding to the inter-association between PCL and phenoxy for entire range of composition. The frequency difference ($\Delta\nu$) between those of free and hydrogen bonded hydroxyl bands can be used as a measure of average strength of hydrogen bonding interaction between individual components. The $\Delta\nu$ values of different hydrogen bonding interactions in phenoxy/PCL-*b*-P2VP blends are given in Table 1.

Table 1
Wavenumber shift in the hydroxyl region for different systems containing phenoxy

System	$\Delta\nu$ (cm^{-1})
Phenoxy	128
Phenoxy/PCL	45[a]
Phenoxy/P2VP	370[b]
Phenoxy/P4VP	192[c]
Phenoxy/PCL-*b*-P2VP	166

[a] Ref. [25].
[b] Ref. [23].
[c] Ref. [26].

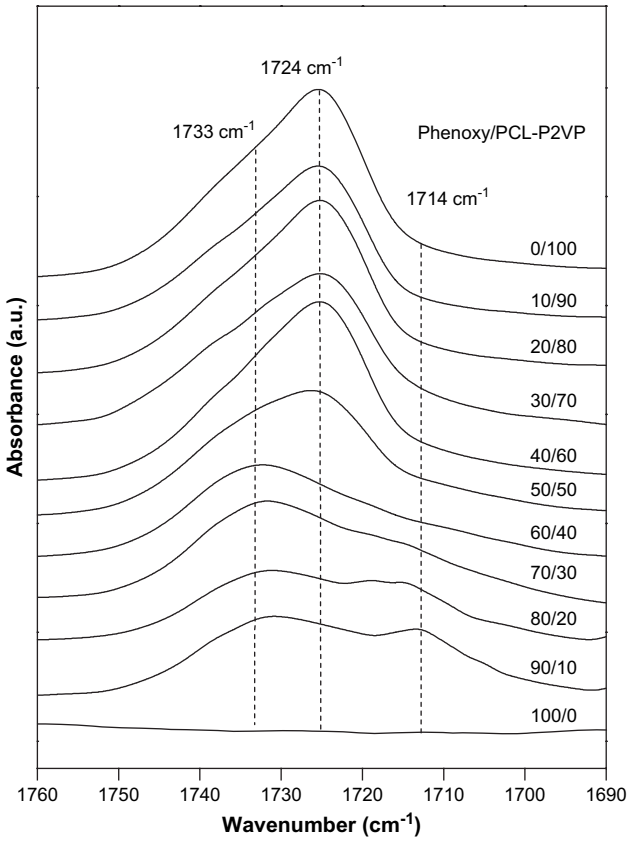

Fig. 3. Carbonyl stretching region of phenoxy/PCL-*b*-P2VP blends at room temperature.

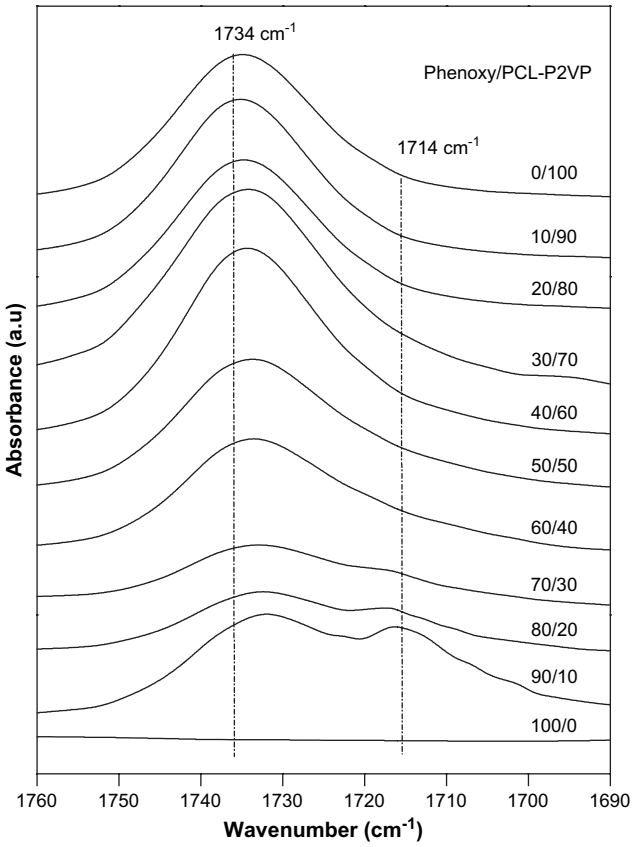

Fig. 4. Carbonyl stretching region of phenoxy/PCL-*b*-P2VP blends at 75 °C.

The $\Delta\nu$ values of phenoxy/PCL and phenoxy/P2VP (or P4VP) binary blends are also given for comparison. It can be observed that the hydrogen bonding interactions between hydroxyl groups in phenoxy and acceptor groups in PCL-*b*-P2VP ($\Delta\nu = 166$) are stronger than the self-association of pure phenoxy ($\Delta\nu = 128\ cm^{-1}$) and phenoxy/PCL blends ($\Delta\nu = 45\ cm^{-1}$) but less than the phenoxy/P2VP (or P4VP) system ($\Delta\nu = 370$ and $196\ cm^{-1}$) [23–26]. Hence it can be suggested that both P2VP and PCL subchains of the block copolymer can interact with phenoxy, but unequally.

The hydrogen bonding formation between phenoxy and PCL blocks of the copolymer can be investigated by analyzing the carbonyl region. The carbonyl region ranging from 1760 to $1700\ cm^{-1}$ in the IR spectra of phenoxy/PCL-*b*-P2VP blends at room temperature is presented in Fig. 3. The spectrum of pure block copolymer shows a sharp peak at $1724\ cm^{-1}$ and a shoulder band at $1733\ cm^{-1}$ corresponding to PCL crystalline and amorphous states, respectively. In phenoxy/PCL-*b*-P2VP blends, as the concentration of phenoxy increases, the crystalline peaks decrease in intensity and eventually disappear at blends containing 60 wt% phenoxy, whereas the amorphous peak increases in intensity and prevails even in blends containing 90 wt% phenoxy. The hydrogen bonding formation between phenoxy and PCL was also examined at 75 °C, above the melting point of PCL and the corresponding IR spectra is given in Fig. 4. The pure PCL shows a single peak at $1733\ cm^{-1}$, corresponding to the amorphous conformation. For phenoxy/PCL-*b*-P2VP blends two peaks were expected, but the amorphous peak is found to be predominant even at high phenoxy concentrations. In general, the number of hydrogen bonds for a given system decreases with increasing temperature due to the negative enthalpy of hydrogen bond formation. On the other hand, the number of hydrogen bonds formed with crystalline/semicrystalline polymer may increase with increasing temperature as the crystalline phase melts progressively. In fact, the peak corresponding to the hydrogen bonding between phenoxy and PCL blocks is expected to be at $1715\ cm^{-1}$ as reported by other authors for phenoxy/PCL binary blends [24]. However, this peak appears only in 80 and 90 wt% phenoxy blends. Hence, it can be concluded that PCL blocks in phenoxy/PCL-*b*-P2VP blends exhibit a weaker ability to form hydrogen bonds with phenoxy at low phenoxy concentrations. This is due to the formation of relatively strong intermolecular hydrogen bonds between phenoxy and P2VP.

The hydrogen bonding between hydroxyl groups of phenoxy and pyridine ring of P2VP can be investigated by examining the IR spectra of the blends in the region 1600–$1550\ cm^{-1}$. The most affected band in this region is at $1590\ cm^{-1}$. As the concentration of phenoxy increases, this band becomes broad and shifts towards higher wavenumber region. This is due to the increase in stiffness of the pyridine ring as a result of hydrogen bonding [27]. The IR spectra corresponding to this region is presented in Fig. 5. The hydrogen bonding interaction between phenoxy hydroxyl groups and

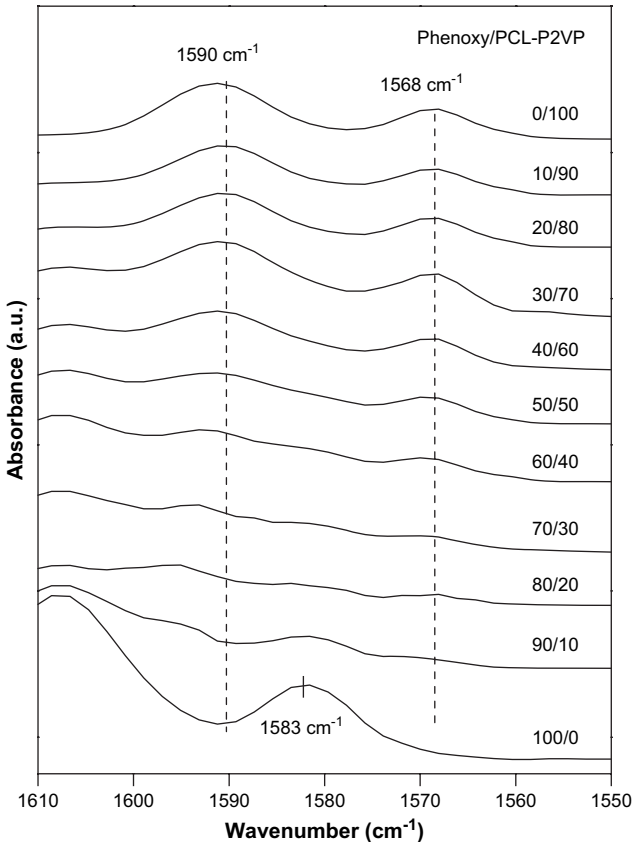

Fig. 5. Infrared spectra corresponding to the wavenumber region 1560–1610 cm^{-1} of phenoxy/PCL-*b*-P2VP blends at room temperature.

pyridine nitrogens is very strong which causes the positive deviation in glass transition temperature of the blends and is discussed in the later part of this article.

The phenoxy/PCL-*b*-P2VP blends were all translucent or transparent above the melting point of PCL and indicates that no macroscopic phase separation had occurred in the blends at a scale exceeding the wavelength of visible light. It is to be noted that, though the inter-association between PCL and phenoxy is relatively weak, the blends comprising these two polymers are miscible. A possible explanation for this can be given based on the free energy of mixing. For a miscible polymer system, the overall free energy of mixing should be zero or less. There is a negative factor from the entropy of mixing, which is generally positive, but relatively small. Even though, the inter-association between PCL and phenoxy is small, it can be assumed that the balance between changes in enthalpy and entropy upon mixing leads to the decrease in free energy of the system, thereby the system becomes miscible [24,28,29].

The quantitative study of fraction of hydrogen bonded carbonyl groups and pyridine groups can be performed with the variation in composition. Since the interaction between phenoxy and PCL blocks in the PCL-*b*-P2VP block copolymer is insignificant, the fraction of hydrogen bonded carbonyl groups was not calculated. The 1568 cm^{-1} band of pyridine ring mode has been taken as the internal standard for calculating the fraction of hydrogen bonded pyridine groups, and included in the curve fitting analysis since it overlaps with the 1590 cm^{-1} band [27]. The fraction of hydrogen bonded pyridine groups can be calculated using the equation:

$$f_b = \frac{A_b/a}{A_b/a + A_f} \quad (1)$$

A_f and A_b are the peak areas of the free and hydrogen bonded pyridine groups. The conversion constant a is the specific absorption ratio of the above two bands. The value of $a = 1$, according to literature for other blends where vinyl pyridines (VP) are mixed with hydrogen donor polymer [27]. The results from curve fitting at room temperature are summarized in Table 2. From the table it can be seen that the fraction of hydrogen bonded pyridine groups increased with increase in phenoxy content.

Table 2
Curve fitting results of phenoxy hydroxyl and P2VP pyridine interactions in phenoxy/PCL-*b*-P2VP blends at room temperature

Phenoxy/PCL-*b*-P2VP	Free pyridine group			Bonded pyridine group			f_b (%)
	ν (cm^{-1})	$W_{1/2}$ (cm^{-1})	A_f (%)	ν (cm^{-1})	$W_{1/2}$ (cm^{-1})	A_b (%)	
90/10	1590	8.2	13.8	1595	14.2	86.2	86.2
80/20	1589	7.8	25.3	1595	15.5	74.7	74.7
70/30	1590	9.8	32	1595	14.8	68.0	68.0
60/40	1590	10.2	37.5	1595	15.5	62.5	62.5
50/50	*1590*	*9.7*	*41.4*	*1595*	*16.2*	*58.6*	*58.6*
40/60	1590	8.3	51.9	1595	16.7	48.1	48.1
30/70	1590	7.9	56.3	1595	15.5	43.7	43.7
20/80	1590	9.3	72.1	1595	14.3	27.9	27.9
10/90	1590	9.2	76.8	1594	15.9	23.2	23.2

From the FTIR results it is confirmed that there is strong intermolecular interactions in phenoxy/PCL-*b*-P2VP blends. The inter-association between phenoxy and block copolymers is found to be higher than the self-association in pure phenoxy. At lower phenoxy contents, the inter-association between phenoxy and P2VP is very strong while PCL shows relatively weaker ability to form hydrogen bonds with phenoxy. Meanwhile, in blends with high phenoxy contents, PCL also forms intermolecular hydrogen bonds with phenoxy, which is confirmed by the appearance of new peaks corresponding to the hydrogen bonded carbonyl groups in the FTIR spectra of the blends.

3.2. Phase behavior and semicrystalline morphology

Thermal behavior of phenoxy/PCL-*b*-P2VP blends was investigated using DSC. Fig. 6 shows DSC curves of the second scan of phenoxy/PCL-*b*-P2VP blends with various compositions. The blends contain a block copolymer PCL-*b*-P2VP with two immiscible blocks, which is supposed to exhibit two T_gs corresponding to PCL blocks and P2VP blocks, respectively. Since both PCL and P2VP were found to be miscible with phenoxy, a change in T_g of both blocks was expected. However, the T_g of PCL blocks is not detectable from the DSC curves under the current experimental conditions. Whereas a single T_g corresponding to phenoxy and P2VP blocks can

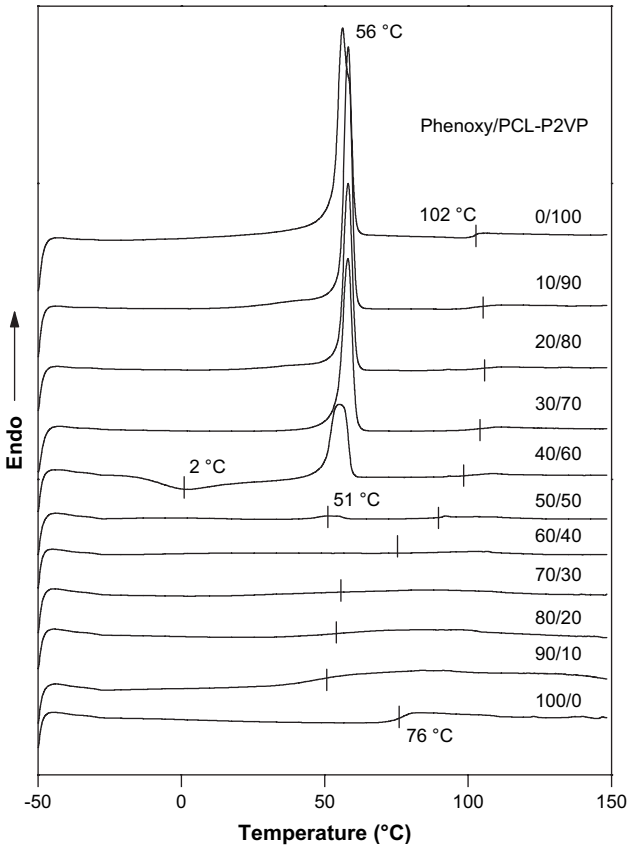

Fig. 6. DSC curves of the second scan of phenoxy/PCL-*b*-P2VP blends.

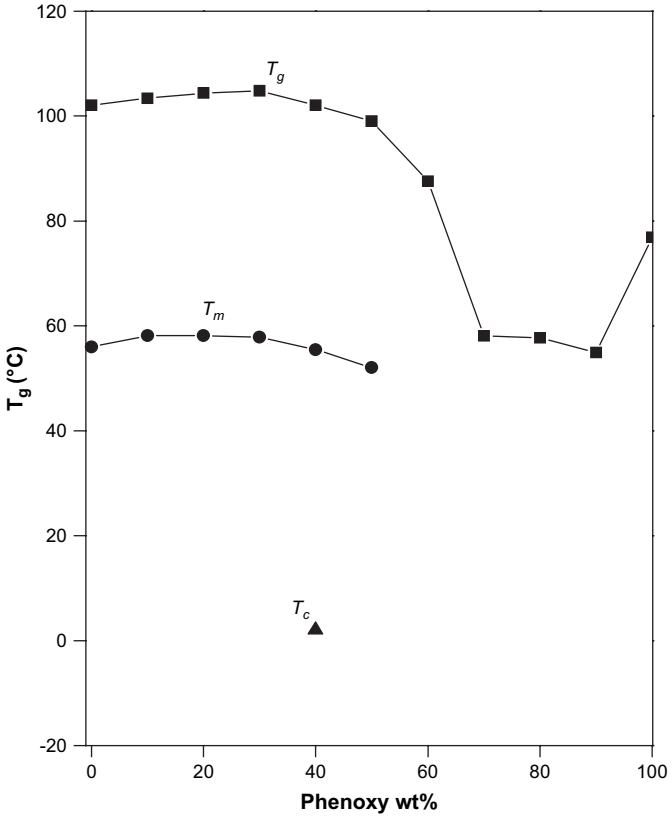

Fig. 7. Thermal transitions during the second scan of phenoxy/PCL-*b*-P2VP blends.

be observed up to 60 wt% phenoxy blends. This can be attributed to the miscibility between these two components due to the formation of strong intermolecular hydrogen bonding. The pure phenoxy exhibits a T_g at 76 °C and that corresponding to P2VP blocks is at 102 °C in the pure block copolymer. The T_g values of the blends are plotted against the composition and is shown in Fig. 7. It can be observed from the figure that the T_g of the blends increases initially with the addition of phenoxy, and the blends exhibit a single T_g higher than that of the individual components (phenoxy and P2VP) up to 60 wt% of phenoxy. In 70 wt% phenoxy blends, T_g value drops below the T_g corresponding to pure phenoxy. The reduction in T_g in blends corresponding to 70 wt% or above phenoxy is due to the dissolution of PCL blocks at these composition. It can be assumed that the positive deviation in T_g of the blends containing up to 60 wt% phenoxy is due to the strong intermolecular hydrogen bonding between phenoxy and P2VP. The reduction in T_g of the blends containing 70 wt% or above phenoxy content is due to the influence of PCL blocks of the block copolymer which start forming hydrogen bonds with phenoxy at these compositions. The formation of intermolecular hydrogen bonds between carbonyl groups of PCL and hydroxyl groups of phenoxy is the basic reason for the miscibility at higher phenoxy contents. It is already evidenced from the FTIR results that there is no significant interaction between PCL and phenoxy in blends containing relatively less phenoxy. However, if the concentration of phenoxy is sufficiently high, PCL can also form hydrogen bonds with phenoxy, regardless of the presence of P2VP. This selective specific interaction has great influence on the microphase morphology of these blends which is described in the later part of this article.

The depression in melting point is a characteristic feature of hydrogen bonded polymer blends [30,31]. The reduction in temperature is caused by the thermodynamic changes due to the reduction in the chemical potential [32]. The pure block copolymer exhibits a melting peak at 55.7 °C which can be crystalline PCL blocks. However, in phenoxy/PCL-*b*-P2VP blends, the melting point remains unchanged with increase in phenoxy content. This indicates that there is no significant interaction between phenoxy and PCL blocks at lower phenoxy concentrations. The melting peak corresponding to PCL crystalline phase reduces in its intensity and eventually disappears at 60 wt% phenoxy content and no melting peaks are observed thereafter. Meanwhile, the blend with 40 wt% phenoxy shows a crystallization exotherm at 2 °C during heating. This indicates that PCL becomes difficult to crystallize, suggesting a gradually decreased crystallization rate.

DSC thermograms of cooling scan of phenoxy/PCL-*b*-P2VP blends are shown in Fig. 8. The pure PCL-*b*-P2VP block copolymer exhibits a crystallization peak at 24 °C, whereas the blends show a crystallization peak higher than that of the block copolymer. Blends containing 40 wt% or above phenoxy has no crystallization peaks, which shows that the crystallization is hindered. The increase in crystallization peak temperature upon the addition of phenoxy may be due to the relaxation of PCL blocks of the block copolymer caused by

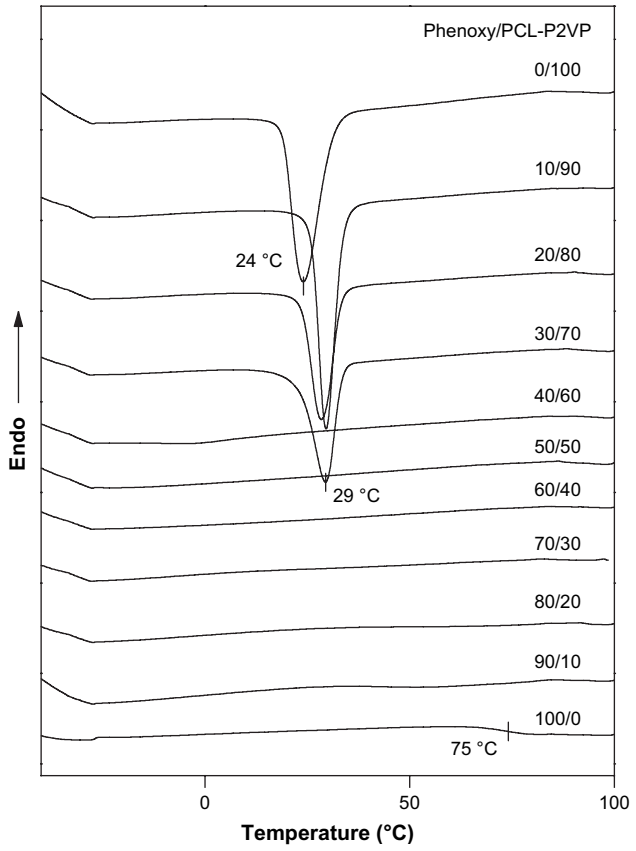

Fig. 8. DSC curves of the cooling scan of phenoxy/PCL-*b*-P2VP blends with different phenoxy concentrations.

the formation of strong hydrogen bonds between P2VP and phenoxy in lower phenoxy content blends.

The semicrystalline morphology of the phenoxy/PCL-*b*-P2VP blends was observed using polarizing optical microscopy. The films of the blends were investigated at different magnifications. The POM images are given in Fig. 9. Pure PCL-*b*-P2VP block copolymer contains PCL crystalline spherulites. In blends, as the concentration of phenoxy increases, the spherulites become smaller and eventually disappear. The blends containing 50 wt% or above phenoxy have no clear indication of crystalline structures, which indicates that the PCL fractions were restricted from crystallization in these compositions.

3.3. Formation of nanostructures in blends

Block copolymers form various ordered morphologies in the size of 10–100 nm. At lower temperatures, most of the block copolymers undergo a microphase separation to form ordered structures. Phase behavior and morphology of diblock copolymers have been intensively studied during the last few years, where different complex, highly ordered structures have been revealed. Binary mixtures of block copolymers with homopolymers can form a rich variety of microstructures including spherical and cylindrical micelles, vesicles, gyroid, and lamellae [10,11]. These microstructures are the result of the spontaneous interfacial areas and curvatures that are established at equilibrium. The average interfacial curvature is highest for spheres and decreases progressively towards planar interfaces in lamellae. In a A-*b*-B/C diblock copolymer/homopolymer system where A rather than B, is strongly solubilized by C, B can form microdomains depending on the concentration.

The phase morphology of the blends was examined using AFM. The AFM phase images of pure block copolymer and blends up to 60 wt% of phenoxy are presented in Fig. 10. Block copolymers composed of incompatible components are known to be self-assembled to form various microphase-separated structures. As expected, pure PCL-*b*-P2VP block copolymer reveals a microphase-separated wormlike morphology as shown in Fig. 10a. The block copolymers possess uniform microphase structure over the whole examined area, with relatively narrow distribution of the microphase size. Upon the

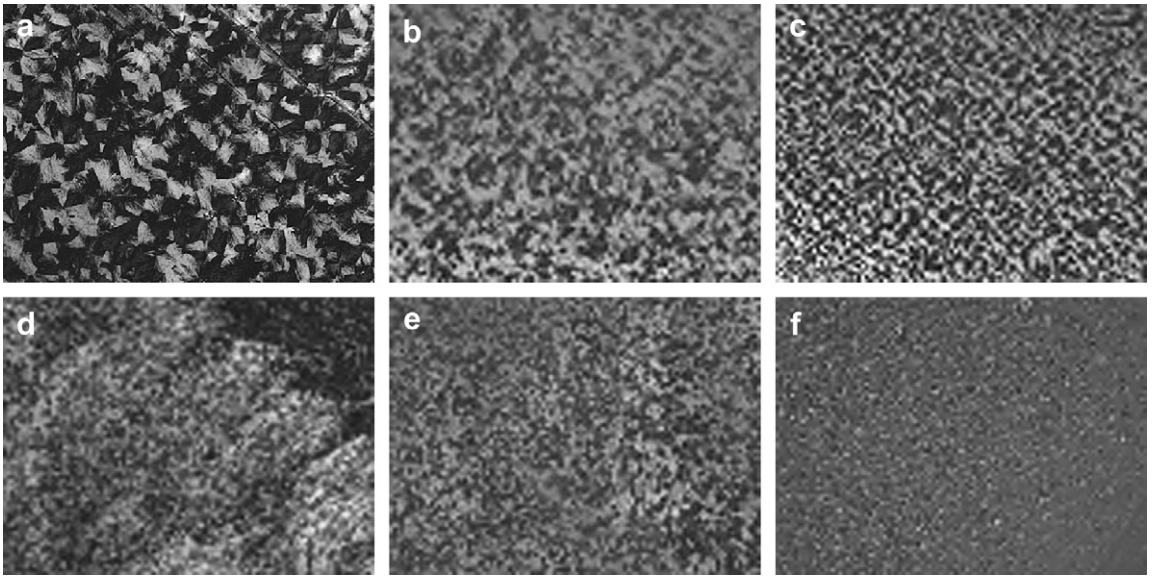

Fig. 9. POM morphologies of phenoxy/PCL-*b*-P2VP blends at room temperature. Phenoxy/PCL-*b*-P2VP: (a) 0/100, (b) 10/90, (c) 20/80, (d) 30/70, (e) 40/60 and (f) 50/50.

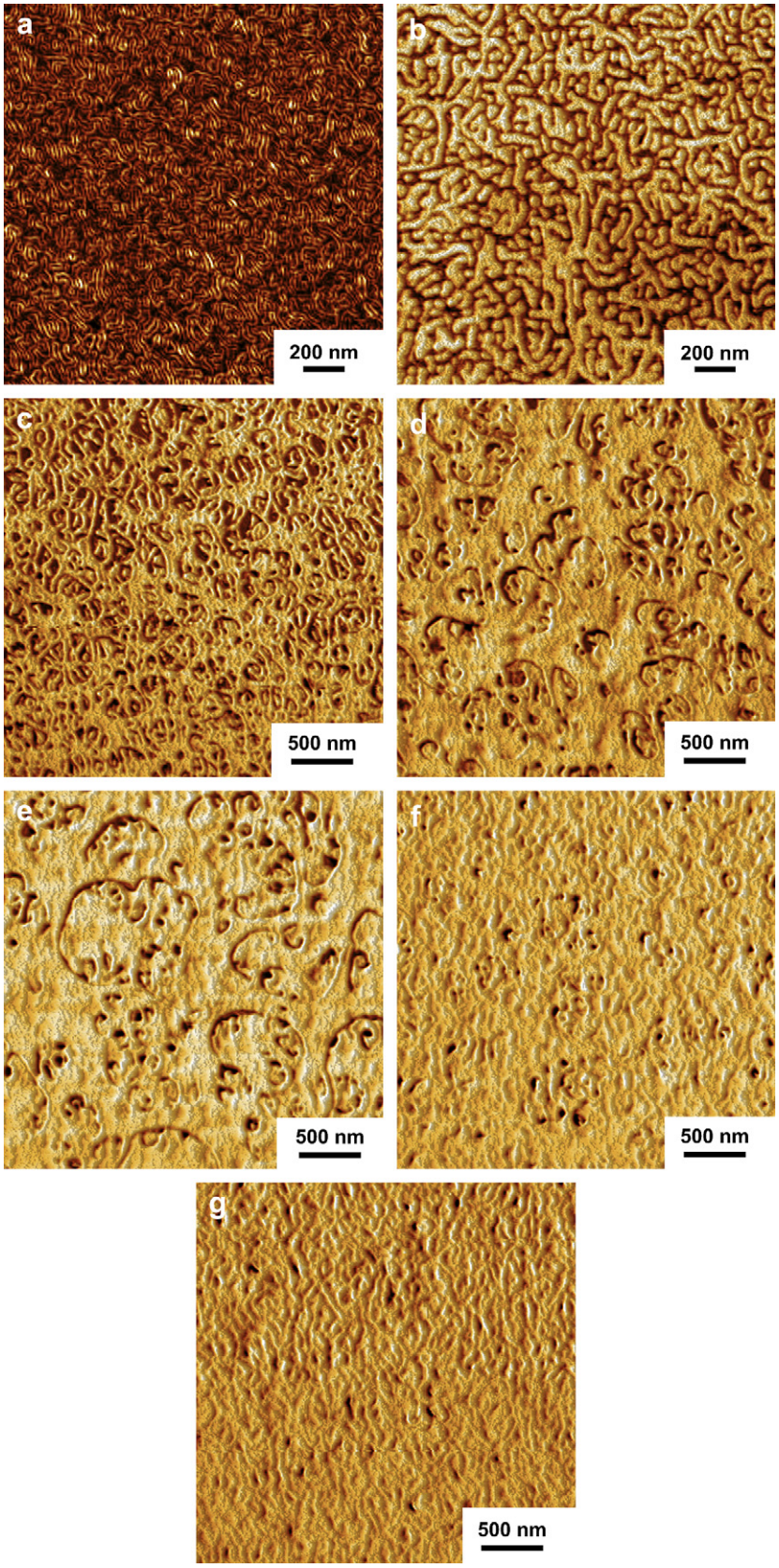

Fig. 10. AFM phase images of phenoxy/PCL-*b*-P2VP blends up to 60 wt% phenoxy. Phenoxy/PCL-*b*-P2VP: (a) 0/100, (b) 10/90, (c) 20/80, (d) 30/70, (e) 40/60, (f) 50/50 and (g) 60/40.

addition of phenoxy, which selectively swells the block copolymer, different morphologies can be observed. It can be seen that blends containing 10 wt% phenoxy exhibit a combined morphology which contains an unusual combination of spherical, cylindrical and wormlike micelles which is given in Fig. 10b. The special feature of this morphology which is to be noted is that their diameters are very uniform, which is calculated to be approximately 40–50 nm. These microstructures are formed as a result of selective swelling of the block copolymer by the phenoxy homopolymer. The microphase morphology of the blends changes with increasing concentration of phenoxy. The assorted morphology changes to typical wormlike microphases when the phenoxy content in the blends rises to 20 wt% (Fig. 10c). The wormlike microphases begin to agglomerate and form hierarchical phase structure in 30 and 40 wt% phenoxy blends (Fig. 10d and e). The microphases with two different length scales, i.e., large microdomains having 300–400 nm size and small wormlike microphases with a size in the order of 40–50 nm, were found outside the large microdomains. As the blend concentration reaches 50–60 wt% phenoxy, the microphases coagulated more and the interface between the microphases becomes less distinct (Fig. 10f and g).

The morphology of the blends undergoes critical changes from 70 wt% phenoxy onwards. The AFM images of phenoxy/PCL-*b*-P2VP blends from 70 wt% and higher phenoxy concentrations are shown in Fig. 11. It is interesting to note that the 70/30 phenoxy/PCL-*b*-P2VP blend shows a bicontinuous morphology, which exhibits a hierarchical nanostructure (Fig. 11a). The hierarchical phase structure shows the structural inhomogeneity at two different nanoscales which consists of spherical microdomains with an average size in diameter of about 15 nm is well dispersed everywhere inside the large microdomains which are in the order of 200–400 nm in size [33]. The morphology of blends containing 80 wt% phenoxy shows a complicated hierarchical microphase-separated structure, wherein the spherical microdomains observed in 70/30 phenoxy/PCL-*b*-P2VP blends coalesce together (Fig. 11b). The morphology of the blends undergoes a rapid transition in 85 wt% phenoxy blends, where a core–shell type of morphology consisting of a phenoxy/P2VP rich phase as core surrounded by a PCL rich shell within a phenoxy/P2VP rich matrix phase was observed (Fig. 11c). So, it can be believed that the core–shell morphology in this 85/15 phenoxy/PCL-*b*-P2VP blends is evolved from the hierarchical structures observed before in 70 wt% phenoxy blends. The hierarchical morphology disappears at 90/10 phenoxy/PCL-*b*-P2VP blends but Fig. 11d shows some microphases with vague interfaces, which means there is still some sort of inhomogeneity present even at this compositions. Finally, blends containing 95 wt% phenoxy exhibit homogenous phase structure consisting of phenoxy, PCL and P2VP as shown in Fig. 11e.

3.4. Mechanism of formation of hierarchical nanostructures

The blends contain a block copolymer P2VP-*b*-PCL and a homopolymer phenoxy which is miscible with both blocks PCL and P2VP. It is known that both PCL and P2VP can form intermolecular hydrogen bonds and exhibit miscibility with phenoxy. It is also proven that the PCL exhibits weak and P2VP exhibits strong intermolecular hydrogen bonding with phenoxy. This imbalance in intermolecular interactions and the repulsion between the two blocks of the block copolymer is the reason for the formation of different microphases in phenoxy/PCL-*b*-P2VP blends.

Pure diblock copolymer exhibited wormlike microphase-separated morphology. In an A-*b*-B diblock copolymer there are two chemically distinct polymer blocks attached together to form a single macromolecule. Block copolymers can self-assemble into a variety of ordered structures by means of microphase separation [11]. This is driven by the enthalpy of demixing of the constituent of the block copolymer. Since these blocks have the general tendency to separate, they exhibit amphiphilic characteristics which is caused by the restriction arise due to the presence of a covalent bond between them, resulting in microphase-separated structures. Blends containing 10 wt% phenoxy exhibit spherical, cylindrical and wormlike swollen microphases. The different microdomains observed in these blends are entirely different from the wormlike microphase of the pure PCL-*b*-P2VP block copolymer, implying that the P2VP blocks are actually swollen with the added phenoxy. The mechanism of formation of different microphases in phenoxy/PCL-*b*-P2VP blends at different compositions is shown in Fig. 12, and corresponding 3D AFM images are also provided. Fig. 12a shows the schematic representation of phenoxy/PCL-*b*-P2VP blends at 10 wt% of phenoxy content. Here, the phenoxy and P2VP blocks of the block copolymer interact very strongly to form one phase. The microphase-separated domains of P2VP segments of a block copolymer show swelling as phenoxy is added. This results in the relative increase in the size of the microdomains of the blends compared to that of the pure block copolymer. The PCL blocks, which are repelled by P2VP, weakly associate with phenoxy at these compositions results in the formation of different microstructures as shown in the figure. The size of these microdomains is calculated to be about 40–50 nm in diameter. In the blends containing 20–60 wt% of phenoxy, the structure of these microdomains changed, which is as the result of segregation of PCL blocks in the blends. The segregation of PCL blocks causes increase in the interfacial area that results in the planar interfaces which form wormlike microstructures and these wormlike structures agglomerate to form different morphologies with increasing phenoxy concentrations. At 30 and 40 wt% phenoxy containing blends, hierarchical nanostructures are observed. These blends exhibit two microdomains at two different length scales, which is due to the segregation of PCL blocks. At 50 or 60 wt% phenoxy blends these structures combine together to form hazy interfaces between the phases.

Hierarchical nanostructures are developed in blends containing 70 wt% or above of phenoxy. It can be seen that 70/30 phenoxy/PCL-*b*-P2VP blends show a typical feature of microphase separation at two different nanoscales. The large

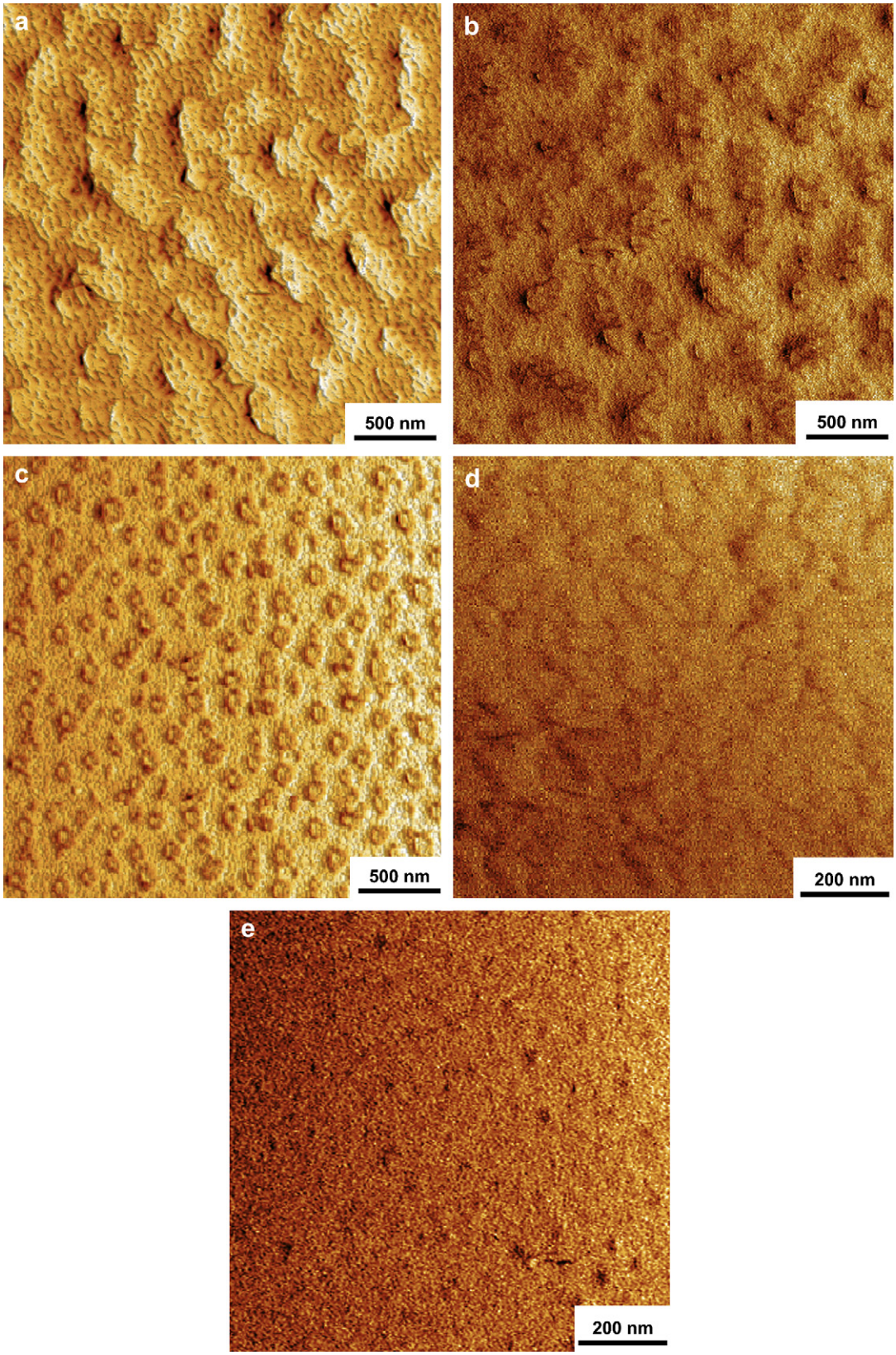

Fig. 11. AFM phase images of phenoxy/PCL-*b*-P2VP blends containing 70 wt% and above phenoxy. Phenoxy/PCL-*b*-P2VP: (a) 70/30, (b) 80/20, (c) 85/15, (d) 90/10 and (e) 95/5.

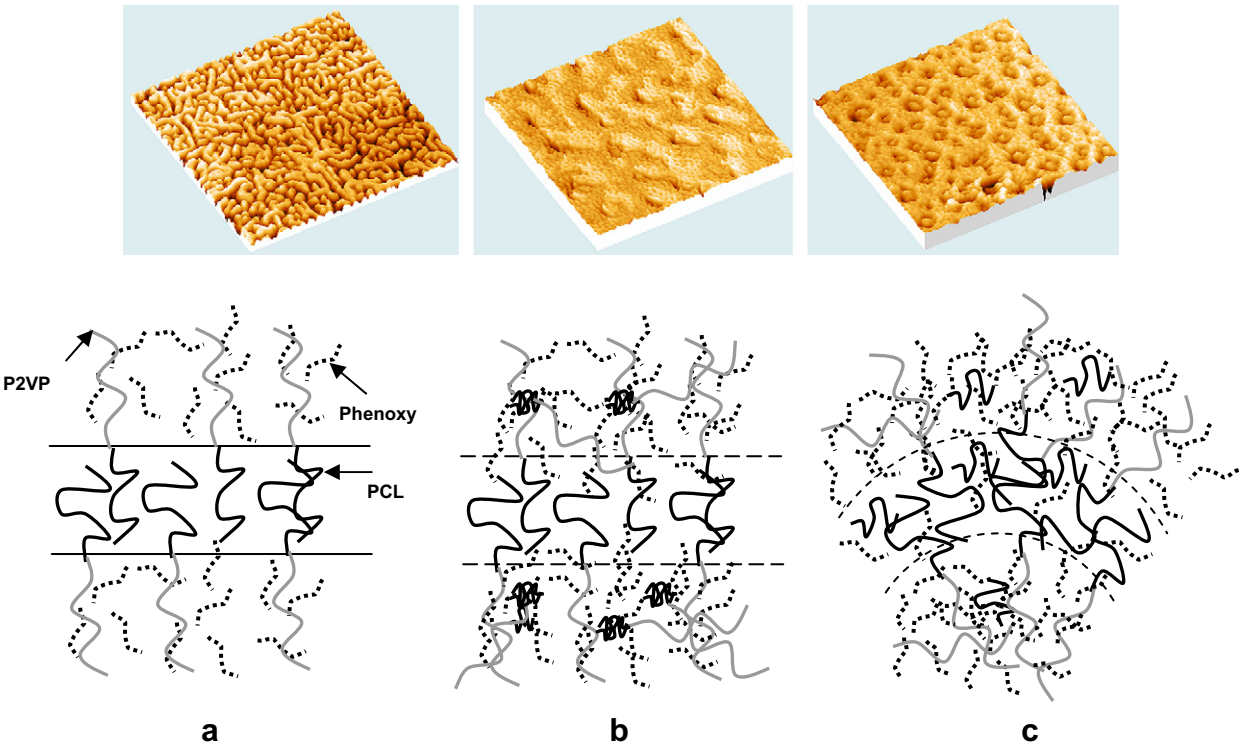

Fig. 12. Schematic representation and 3D AFM images of different microphases in phenoxy/PCL-*b*-P2VP blends: (a) cylindrical and wormlike microdomains at 10 wt%, (b) hierarchical nanostructure at 70 wt% and (c) core–shell phase structure at 85 wt% phenoxy concentrations.

dispersed microdomains (200–400 nm in size) with internal spherical microdomain structure (15 nm) can be observed. This is schematically represented in Fig. 12b. It can be proposed that the formation of hierarchical nanostructures at this composition is as a result of PCL blocks which started some intermolecular interaction with phenoxy. This hierarchical structure is quite different from that observed in 30 or 40 wt% phenoxy blends, where the PCL blocks were segregated completely from the phenoxy/P2VP single phase. However, it is obvious that in 70 wt% phenoxy blends, the amount of phenoxy is relatively high. Though there exists a strong interaction between P2VP and phenoxy, the increased amount of phenoxy at these compositions results in some fraction of free hydroxyl groups that are available for hydrogen bonding with carbonyl groups of PCL. This interaction is not sufficient to bring about a homogeneous system. But this relatively negligible amount of hydrogen bonding between PCL and phenoxy causes the formation of some PCL rich phase (15 nm) inside the phenoxy/P2VP rich phase which already forms microphases in the order of 200–400 nm. This structural hierarchy can be well identified from the schematic representation of hierarchical nanostructures obtained in 70/30 phenoxy/PCL-*b*-P2VP blends.

As the concentration of phenoxy increases again, the internal spherical microdomains segregate to form featureless microstructures as observed in 80/20 phenoxy/PCL-*b*-P2VP blends. The microphase morphology changed again into a core–shell microstructure in the blends containing 85 wt% phenoxy. This core–shell microstructure, in which a miscible phenoxy/P2VP rich phase forms the core and PCL rich phase forms the shell, are dispersed in a matrix of miscible phenoxy/P2VP rich phase. The schematic representation of core–shell morphology is shown in Fig. 12c. This is supposed to be due to the increased interaction between PCL and phenoxy at these compositions which make the PCL to be segregated to form a PCL rich shell outside the core of phenoxy/P2VP rich phase. In 90/10 phenoxy/PCL-*b*-P2VP blends the phase almost disappears, but still a PCL rich microphase can be observed between phenoxy/P2VP rich phase. The interface between the phases is ambiguous, which indicate that majority of PCL blocks are miscible in the phenoxy phase and the blend is on the margin of a homogeneous system which is observed in 95/5 phenoxy/PCL-*b*-P2VP blends.

The formation of hierarchical nanostructures in blends containing 70 wt% or above phenoxy is assumed to be due to the increased intermolecular interaction between PCL and phenoxy which can be further confirmed by the FTIR spectra of this compositions and is shown in Fig. 13. It can be seen from the figure that the peak at 1714 cm^{-1} corresponding to the hydrogen bonded carbonyl groups increases in intensity at higher phenoxy concentrations. The increase in hydrogen bonding is due to the availability of free hydroxyl groups since the concentration of phenoxy is relatively very high compared to the block copolymer. At this stage phenoxy, which behaved as a selective solvent for P2VP at lower phenoxy concentrations, acts as a common solvent for both segments of the block copolymer results in a homogeneous system at 95 wt% phenoxy blends.

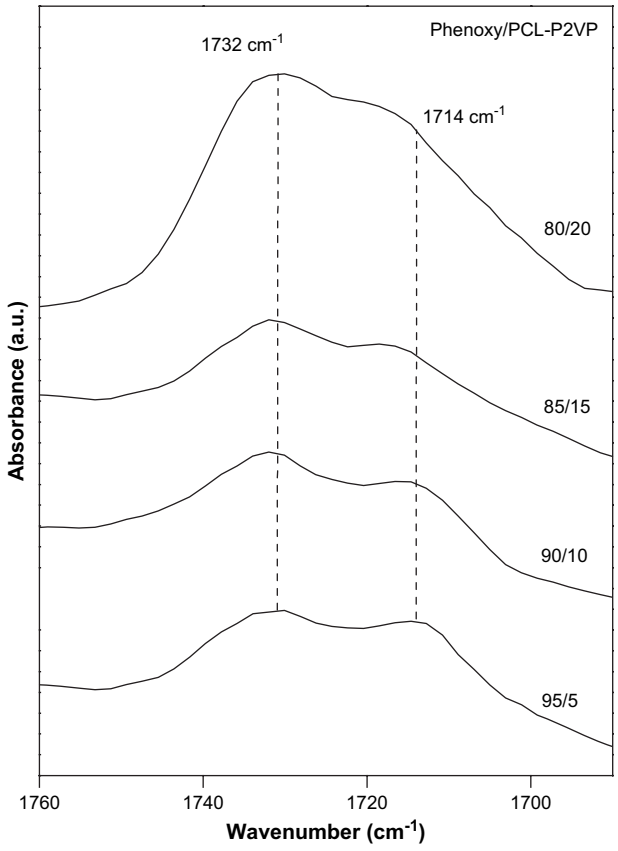

Fig. 13. Carbonyl stretching region of phenoxy/PCL-*b*-P2VP blends containing 80 wt% and above phenoxy at room temperature.

4. Conclusions

We have successfully investigated the selective hydrogen bonding in phenoxy and PCL-*b*-P2VP block copolymer blends. The FTIR results provide clear evidence for the existence of hydrogen bonds in the blends at different compositions. At low compositions, phenoxy forms a strong hydrogen bond with P2VP and thus acts as a selective solvent for PCL-*b*-P2VP block copolymer. However, at higher compositions, PCL also forms hydrogen bonds with phenoxy hydroxyls which results in a homogeneous system. So at higher compositions phenoxy acts as a common solvent for the block copolymer. From FTIR results it is obvious that hydrogen bonding between PCL and phenoxy exists only in 70 wt% or above phenoxy containing blends. The DSC results also give evidence for the miscibility of the PCL phases at higher phenoxy concentrations. The selective solubility of the amphiphilic block copolymer by phenoxy leads to the formation of a variety of composition dependent microphase morphologies including hierarchical nanostructures in phenoxy/PCL-*b*-P2VP blends. At lower phenoxy contents, the selective swelling of the block copolymer by phenoxy leads to the formation of wormlike microphases. With higher phenoxy contents in the blends, hierarchical and core–shell morphologies were obtained owing to the formation of intermolecular hydrogen bonding between phenoxy and PCL at higher phenoxy compositions.

Acknowledgments

This work was financially supported by the Australian Research Council under the Discovery Project Schemes and by Deakin University through a CRGS grant. One of us (N.H.) would like to express his gratitude for a DUIRS scholarship from Deakin University.

References

[1] Yuichi M, Takeshi K, Shusaku N, Takahiro S. Chem Mater 2007; 19:1540.
[2] Asari T, Arai S, Takano A, Matsushita Y. Macromolecules 2006;39:2232.
[3] Lefèvre N, Fustin CA, Varshney SK, Gohy JF. Polymer 2007;48:2306.
[4] Park M, Harrison C, Chaikin PM, Register RA, Adamson DH. Science 1997;276:1401.
[5] Muthukumar M, Ober CK, Thomas EL. Science 1997;27:1225.
[6] Guo Q, Thomann R, Gronski W, Staneva R, Ivanova R, Stühn B. Macromolecules 2003;36:3635.
[7] Kataoka K, Harada A, Nagasaki Y. Adv Drug Delivery Rev 2001;47:113.
[8] Savic R, Luo LB, Eisenberg A. Science 2003;300:615.
[9] Nobuhiro N, Kazunori K. Adv Polym Sci 2006;193:67.
[10] Hamley IW. Block copolymers. Oxford: Oxford University Press; 1999.
[11] Bates FS, Fredrickson GH. Phys Today 1999;52:33.
[12] Antonietti M, Conrad J, Thünemann A. Trends Polym Sci 1997;5:262.
[13] Mogi Y, Nomura M, Kotsuji H, Ohnishi K, Matsushita Y, Noda I. Macromolecules 1994;27:6755.
[14] Gido SP, Schwark DW, Thomas EL, Goncalves MC. Macromolecules 1993;26:2636.
[15] Stadler R, Auschra C, Beckmann J, Krappe U, Voigt-Martin I, Leibler L. Macromolecules 1995;28:3080.
[16] Ruokolainen J, Saariaho M, Ikkala O, ten Brinke G, Thomas EL, Torkkeli M, et al. Macromolecules 1999;32:1152.
[17] Ruokolainen J, Mäkinen R, Torkkeli M, Mäkelä T, Serimaa R, ten Brinke G, et al. Science 1998;280:557.
[18] Abetz V, Goldacker T. Macromol Rapid Commun 2000;21:16.
[19] Hammouda B. Adv Polym Sci 1993;106:87.
[20] Hashimoto T, Kimishima K, Hasegawa H. Macromolecules 1991; 24:5704.
[21] Hashimoto T, Izumitani T, Oono K. Makromol Chem Macromol Symp 1995;98:925.
[22] Zhao JQ, Pearce EM, Kwei TK. Macromolecules 1997;30:7119.
[23] de Ilarduya AM, Eguiburu JL, Espi E, Iruin JJ, Fernhdez-Berridi MJ. Makromol Chem 1993;194:501.
[24] Coleman MM, Moskala EJ. Polymer 1983;24:251.
[25] Kuo SW, Huang CF, Chang FC. J Polym Sci Part B Polym Phys 2001;39:1348.
[26] Zheng S, Mi M. Polymer 2003;44:1067.
[27] Cesteros LC, Meaurio E, Katime I. Macromolecules 1993;26:2323.
[28] Guo Q, Zheng H. Polymer 1999;40:637.
[29] Zhong Z, Guo Q. Polymer 1997;38:279.
[30] Zhong Z, Guo Q. Polymer 1998;3:517.
[31] Zheng H, Zheng S, Guo Q. J Polym Sci Part A Polym Chem 1997; 35:3161.
[32] He Y, Zhu B, Inoue Y. Prog Polym Sci 2004;29:1021.
[33] Guo Q, Thomann R, Gronski W, Thurn-Albrecht T. Macromolecules 2002;35:3133.